

We are IntechOpen, the world's leading publisher of Open Access books Built by scientists, for scientists

6,900

Open access books available

186,000

International authors and editors

200M

Downloads

Our authors are among the

154

Countries delivered to

TOP 1%

most cited scientists

12.2%

Contributors from top 500 universities



WEB OF SCIENCE™

Selection of our books indexed in the Book Citation Index
in Web of Science™ Core Collection (BKCI)

Interested in publishing with us?
Contact book.department@intechopen.com

Numbers displayed above are based on latest data collected.
For more information visit www.intechopen.com



Human-in-the-Loop Control for a Broadcast Camera System

Rares Stanciu and Paul Oh
Drexel University
USA

1. Introduction

There are many tools that carry cameras. Their working domain is usually surveillance, surface inspection, and broadcasting. Devices like rovers, gantries, and aircrafts often possess video cameras. The task is usually to maneuver the vehicle and position the camera to obtain the desired fields-of-view. A platform widely used in the broadcasting industry can be seen in Figure 1. The specific parts are usually the tripod, the boom, and the motorized pan-tilt unit (PTU).

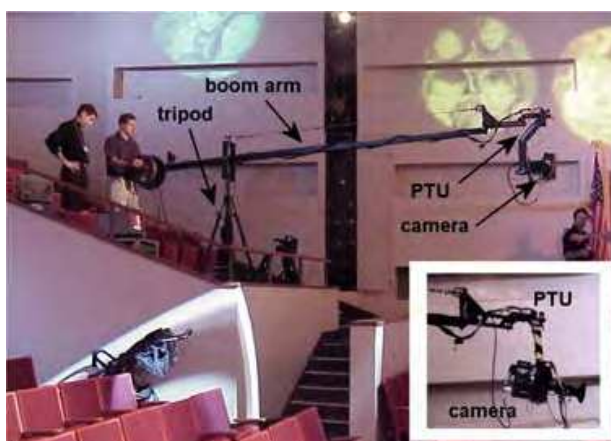


Fig. 1. The operator can move the boom horizontally and vertically to position the camera. The pan-tilt (*lower right inset*) head provides additional DOFs.

Manual operation of such a tool requires two skilled operators. Typically, one person will handle the boom while the second operator will coordinate the PTU camera to track the subjects using two joysticks. Tracking the moving objects is difficult because there are many degrees-of-freedom (DOFs) to be coordinated simultaneously. Increasing the target's speed increases the tracking difficulty. Using computer vision and control techniques ensures the automatic camera tracking and reduces the number of DOFs the operator has to coordinate. This way the platform can be operated by one person concentrating only on the booming. The use of such techniques enables the tracking of faster moving objects.

Searching through the literature on this subject reveals that there is a wealth of existing research in the visual servoing domain. An excellent starting point in the literature search is (Hutchinson et al., 1996). Extensive research is described in (Corke & Good, 1996); (Hill &

Source: Visual Servoing, Book edited by: Rong-Fong Fung,
ISBN 978-953-307-095-7, pp. 234, April 2010, INTECH, Croatia, downloaded from SCIYO.COM

Park, 1973); (Oh & Allen, 2001); (Oh, 2002); (Sanderson & Weiss, 1980); (Stanciu & Oh, 2002); (Stanciu & Oh, 2003); (Papanikolopoulos et al., 1993). It is to be noted that in these publications, researchers have dealt completely with automated hardware (where no operator is involved). The system described in this paper is operated by humans. Some of the seminal man-machine interface work is represented by (Sheridan & Ferrell, 1963); (Ferrier, 1998); (Fitts, 1954).

The system utilized for experimentation is shown in Figure 2. The platform is composed of a four-wheeled dolly, boom, motorized PTU, and camera. The dolly can be pushed and steered. The 1.2-m-long boom is linked to the dolly via a cylindrical pivot that allows the boom to sweep horizontally (pan) and vertically (tilt). Mounted on one end of the boom is a two-DOF motorized PTU and a video camera weighing 9.5 kg. The motors allow an operator to both pan and tilt the camera 360° at approximately 90°/sec. The PTU and the camera are counterbalanced by a 29.5-kg dumbbell mounted on the boom's opposite end.

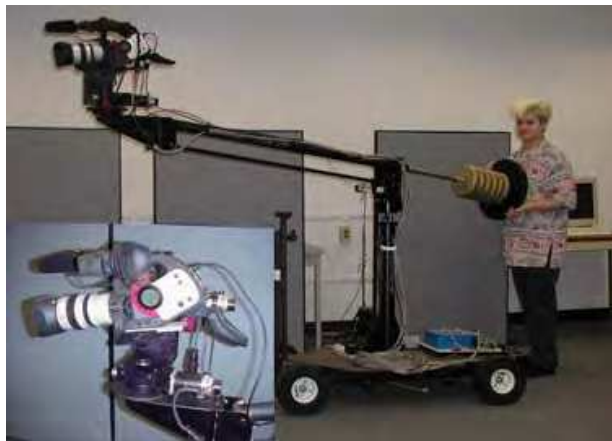


Fig. 2. The operator can boom the arm horizontally and vertically to position the camera. The pan-tilt head (*lower left inset*) provides additional DOFs.

Use of this boom-camera system normally entails one or more skilled personnel performing three different operations.

1. With a joystick, the operator servos the PTU to point the camera. A PC-104 small board computer and an ISA bus motion control card allow for accurate and relatively fast camera rotations.
2. The operator physically pushes on the counterweighted end to boom the camera horizontally and vertically. This allows one to deliver a diverse range of camera views (e.g. shots looking down at the subject), overcomes PTU joint limitations, and captures occlusion-free views.
3. The operator can push and steer the dolly in case the boom and PTU are not enough to keep the target image in the camera's desired field-of-view.

Tracking a moving object using such a tool is a particularly challenging task. Tracking performance is thus limited to how quickly the operator manipulates and coordinates multiple DOFs. Our particular interest in computer vision involves improving the camera operator's ability to track fast-moving targets. By possessing a mechanical structure, actuators, encoders, and electronic driver, this boom is a mechatronic system. *Visual-servoing* is used to control some DOFs so that the operator has fewer joints to manipulate.

This paper describes the implementation of several controllers in this human-in-the-loop system and discusses quantitatively the performance of each. The CONDENSATION

algorithm is used for the image processing. As this algorithm is described in some publications (Isard & Blake, 1998), this paper will not focus on the image processing. Section 2 describes the experimental setups used. The controllers are described in Section 3. Development and validation of a boom-camera model is also presented. Section 4 describes a comparison between a well skilled operator versus a novice, both with and without the visual servoing. Section 5 presents the conclusions.

2. Experimental setups

The „artistic“ side of a film shooting scenario is often very important. Because they involve humans, these scenarios are (strictly speaking) not repeatable. Therefore, to compare the behavior of different controllers, an experimental framework is needed. As such, the experiments were designed to offer the best possible answers for both scientific and artistic community.

The first experiment was people-tracking. A person was asked to walk in the laboratory. The camera attempted tracking while an operator boomed. Figure 3 (a) shows such an experiment.

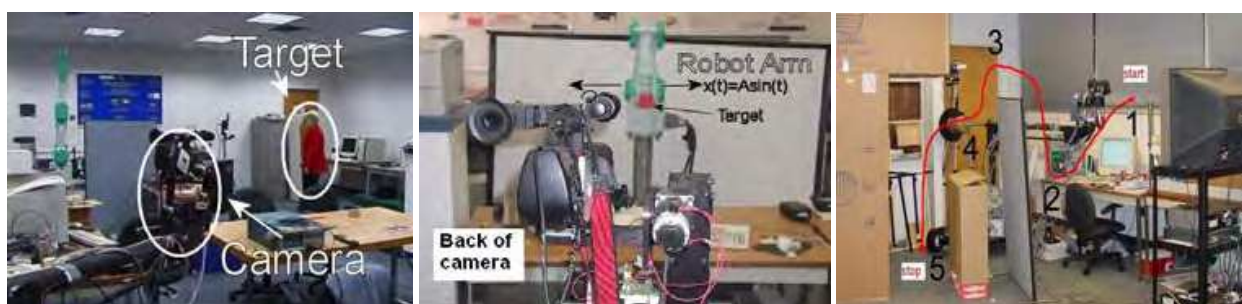


Fig. 3. (a) Typical people-tracking set-up. A subject walks around and the camera attempts tracking while booming. (b) Wooden block target was mounted on the end-effector of a Mitsubishi robot arm (*background*). The boom-camera system (*foreground*) attempts to keep the target's image centered in the camera's field-of-view. (c) Novice and a well-skilled operator will manipulate the boom appropriately to move the camera along the shown path, with and without the help of the visual servoing. In addition to booming, under manual control, the operator will also have to coordinate camera's two DOFs using a joystick. Visual servoing tracking error is recorded for comparison.

Each new designed controller attempted to increase tracking performance. The second experiment was developed in an attempt to design a metric for performance. A Mitsubishi robotic arm was instructed to sinusoidally move the target back and forth [Figure 3 (b)]. While the operator boomed, the camera tracked the target. Target motion data, error, and booming data were recorded during the experiments and plotted for comparison with previous results.

At this point, it was interesting to determine whether the vision system was usable in sport broadcasting. An experiment in which the camera tried to track a ball moving between two people was set up. The experiment showed successful tracking but highlighted some challenges. This setup is described in Section 3.8.

Once the camera was considered to ensure a satisfactory tracking performance, it was interesting to determine how it can help the operator. To answer this question, another experiment was designed. Again, the Mitsubishi robotic arm was used. This time, the robot

moved the target on a trajectory corresponding to the number “8”. A novice and an experienced operator boomed along a predefined path and attempted tracking the robot end-effector with and without vision. Figure 3(c) shows the way the operator should boom. The visual servoing tracking error was recorded and plotted. This experiment is described in Section 4.

3. Controllers description

This section presents the hypotheses, describes the controllers in detail, and discusses the experiments and results during this research.

3.1 Proportional controller

To establish a base level, the first of our hypotheses was launched. It states that by *using a very simple controller (proportional) and a very simple image processing technique (color tracking), the camera is able to track a moving target when booming.*

The proportional controller was implemented. The current target position in the image plane is compared with the desired position and an error signal is generated. This error signal will determine the speed of the camera in its attempt to bring the target in focus. The controller gain K_x was set to 100. People-tracking experiment was attempted using this controller [Figure 3(a)]. A person wearing a red coat was asked to walk in the laboratory. The color-tracker board was trained for red. The task was to keep the red coat in the camera's field of view while an operator boomed. In this experiment, the camera-target distance was about 5 m.

To assess the controller performance quantitatively a toy-truck was to be tracked. An artificial white background was used to help the vision system to detect the target. In this experiment, the camera-target distance was 3 m. The toy moved back and forth while the camera attempted tracking. Camera motion data, booming data, and tracking error were recorded. The plots can be seen in Figure 4. Figure 4(a) shows the pan motor encoder indication, (b) shows the error (in pixels), and (c) shows the booming angle (in degrees). It can be seen that as the operator is booming and the target is moving, the controller performs a visually servoed counterrotation. The system was able to track the moving target even when using a very simple controller. Still, as one expects, there were two challenges: system stability and tracking performance.

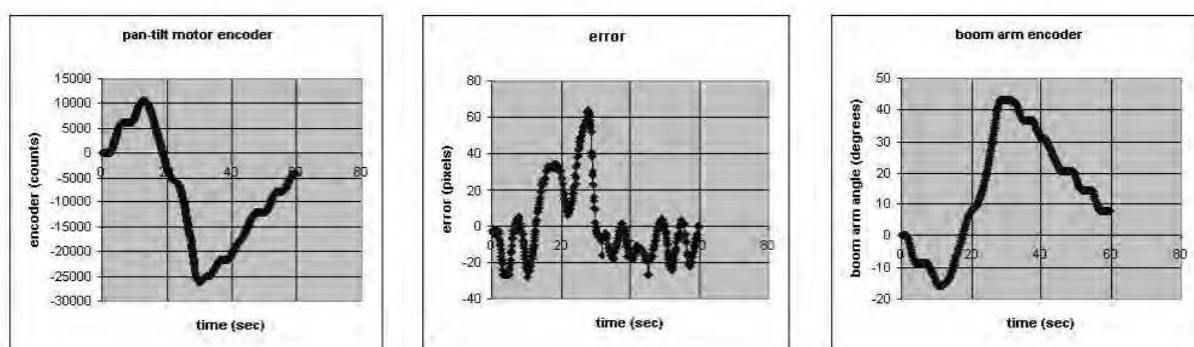


Fig. 4. $K_x = 100$ (a) PTU motor encoder. (b) Pixel error. (c) Boom-arm encoder.

The experiments have demonstrated that the key design parameter, when visually servoing redundant DOF systems, is stability, especially when the target and the boom move 180° out

of phase. If boom motion data is not included, camera pose cannot be determined explicitly because there are redundant DOFs. As a result, the system could track a slow-moving target rather well, but would be unstable when the target or boom moves quickly.

The second issue was the tracking performance. With the proportional controller, the operator boomed very slowly (less than $1^\circ/\text{sec}$). The target also moved slowly (about 10 cm/s). Any attempt to increase the booming or target speed resulted in the tracking failure. Both the experiments proved the first hypothesis. It is important to underline that the vision had no information about booming. Introducing booming information could improve tracking performance as well as stability.

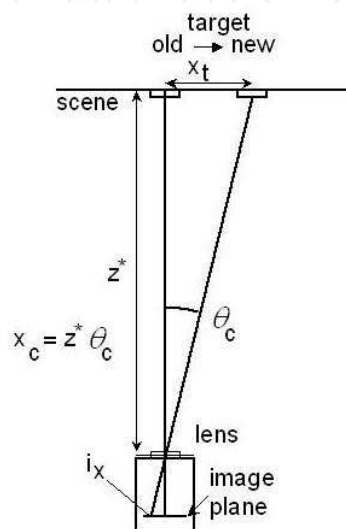


Fig. 5. Schematic of camera scene

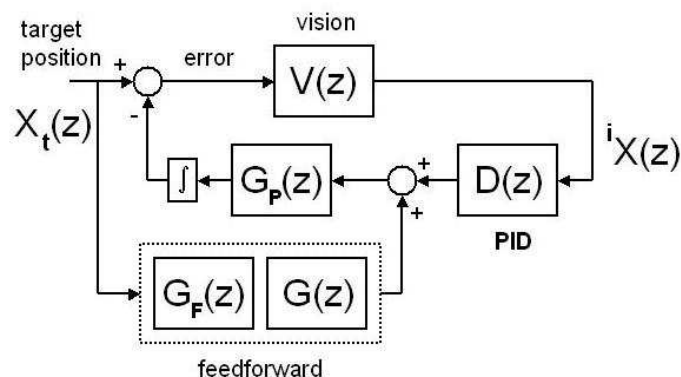


Fig. 6. Feedforward controller with a feedback compensation.

3.2 Feedforward controller

The second hypothesis was that *by using a feedforward control technique, we can improve both the performance and the stability*. A feedforward controller was designed to validate the second hypothesis. This controller provides the target motion estimation (Corke & Good, 1996). Figure 6 depicts a block diagram with a transfer function

$$\frac{iX(z)}{X_t(z)} = \frac{V(z)(1 - G_p(z)D_F(z))}{1 + V(z)G_p(z)D(z)} \quad (1)$$

where ${}^iX(z)$ is the position of the target in the image, $X_t(z)$ is the target position, $V(z)$ and $G_p(z)$ are the transfer functions for the vision system and PTU, respectively. The previous and actual positions of the target in the image plane are used to predict its position and velocity one step ahead. Based on this, the feedforward controller will compute the camera velocity for the next step. $D_f(z) = G_f(z)G(z)$ represents the transfer function of the filter combined with the feedforward controller. $D(z)$ is the transfer function for the feedback controller. If $D_f(z) = G_p^{-1}(z)$, the tracking error will be zero, but this requires knowledge of the target position that is not directly measurable. Consequently, the target position and velocity are estimated. For a horizontally translating target, its centroid in the image plane is given by the relative angle between the camera and the target

$${}^iX(z) = K_{lens} (X_t(z) - X_r(z)) \quad (2)$$

where ${}^iX(z)$ and $X_t(z)$ are the target position in the image plane and world frame, respectively. $X_r(z)$ is the position of the point that is in the camera's focus (due to the booming and camera rotation) and K_{lens} is the lens zoom value. The target position prediction can be obtained from the boom and the PTU, as seen in Figure 5. Rearranging this equation yields

$$\hat{X}_t(z) = \frac{{}^i\tilde{X}(z)}{K_{lens}} + X_r(z) \quad (3)$$

where \hat{X}_t is the predicted target position.

3.3 The $\alpha - \beta - \gamma$ filter

Predicting the target velocity requires a tracking filter. Oftentimes, a Kalman filter is used, but is computationally expensive. Since Kalman gains often converge to constants, a simpler $\alpha - \beta - \gamma$ tracking filter can be employed that tracks both position and velocity without steady-state errors (Kalata & Murphy, 1997); (Tenne & Singh, 2000). Tracking involves a two step process. The first step is to predict the target position and velocity

$$x_p(k+1) = x_s(k) + Tv_s(k) + T^2a_s(k) / 2 \quad (4)$$

$$v_p(k+1) = v_s(k) + Ta_s(k) \quad (5)$$

where T is the sample time and $x_p(k+1)$ and $v_p(k+1)$ are the predictions for the position and velocity at iteration $k+1$, respectively. The variables $x_s(k)$, $v_s(k)$, and $a_s(k)$ are the corrected (smoothed) values of iteration k for position, velocity, and acceleration, respectively. The second step is to make corrections

$$x_s(k) = x_p(k) + \alpha(x_o(k) - x_p(k)) \quad (6)$$

$$v_s(k) = v_p(k) + (\beta/T)(x_o(k) - x_p(k)) \quad (7)$$

$$a_s(k) = a_p(k-1) + (\gamma/2T^2)(x_o(k) - x_p(k)) \quad (8)$$

where $x_o(k)$ is the observed (sampled) position at iteration k . The appropriate selection of gains α , β , and γ will determine the performance and stability of the filter (Tenne & Singh 2000). The $\alpha - \beta - \gamma$ filter was implemented to predict the target velocity in the image plane with gains set at $\alpha = 0.75$, $\beta = 0.8$, and $\gamma = 0.25$. This velocity was, then, used in the feedforward algorithm, as shown in Figure 7. Image processing in the camera system can be modeled as a $1/z$ unit delay that affects the camera position x_c , and estimates of the target position. In Figure 7, the block $G_F(z)$ represents the transfer function of the $\alpha - \beta - \gamma$

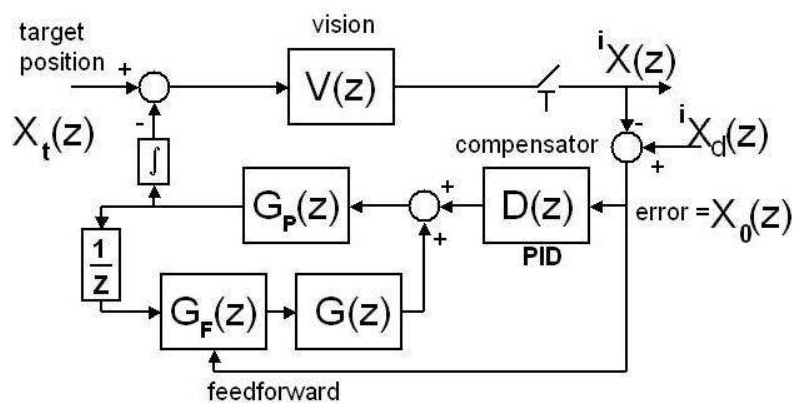


Fig. 7. Feedforward controller with a feedback compensation as it was implemented

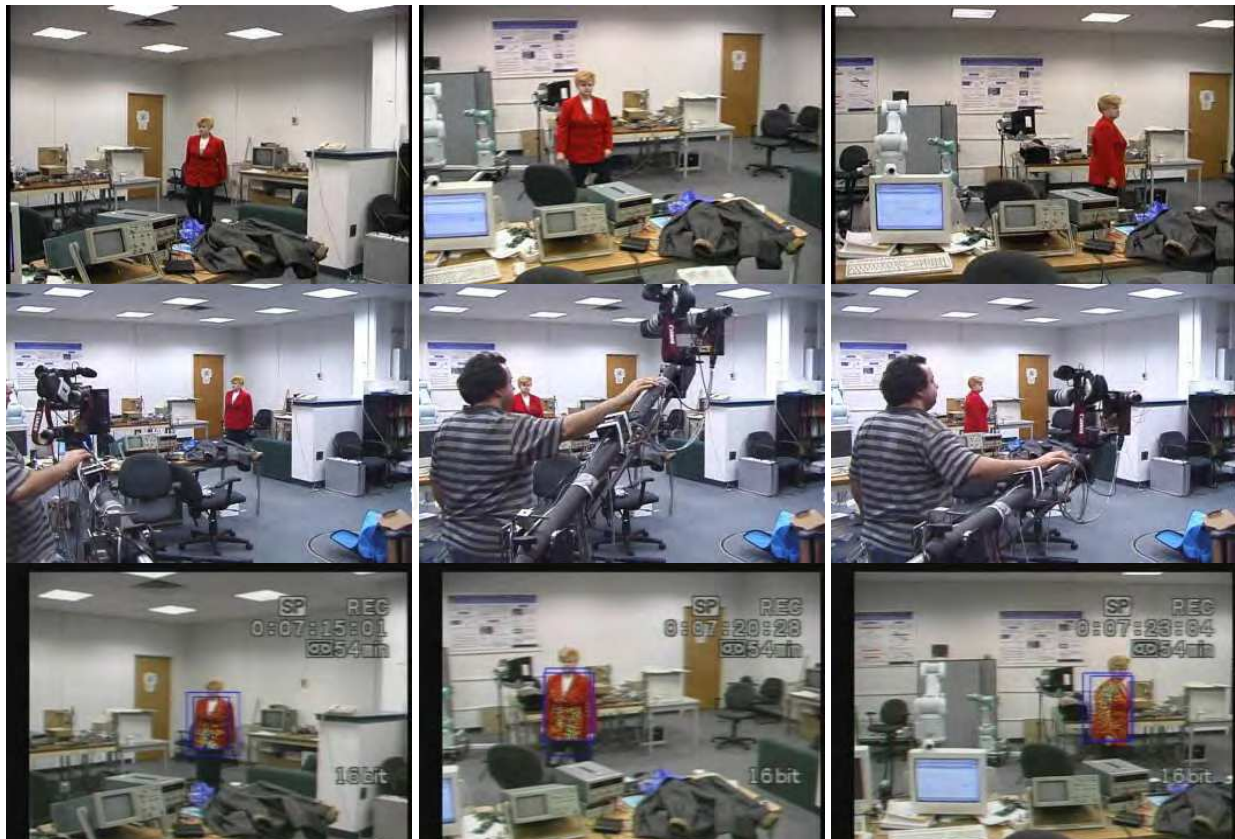


Fig. 8. Three sequential images from videotaping the feedforward controller experiment. Camera field-of-view shows target is tracked *top row*. Boom manually controlled *middle row*. Working program *bottom row*.

filter, with the observed position as the input and the predicted velocity as the output. $X_d(z)$ represents the target's desired position in the image plane and its value is 320 pixels. $X_o(z)$ represents the position error in the image plane (in pixels).

The constant K_{lens} converts pixels in the image plane to meters. K_{lens} was assigned a constant value, and it assumes a pinhole camera model that maps the image plane and world coordinates. This constant was experimentally determined by comparing the known lengths in world coordinates to their projections in the camera's image plane. With the system equipped with the feedforward controller, a couple of experiments were performed. Again, the first was the people-tracking experiment. A subject was asked to walk back and forth in the laboratory environment. The operator boomed while the camera tracked the subject. Sequential images from the experiment can be seen in Figure 8. The first row shows the boom camera view. It can be seen that the system is not in danger of losing the target. The second row shows the operator booming while the third row shows the program working. It can be seen that the target is well detected.

To quantitatively assess the performance, the Mitsubishi robotic arm was instructed to move the target sinusoidally. The camera was instructed to track this target using the proportional as well as the feedforward controller. An operator panned the boom at the same time. Data regarding Mitsubishi motion, booming motion, and tracking error were recorded. The performance is assessed by comparing the tracking error. The setup can be seen in Figure 3(b).

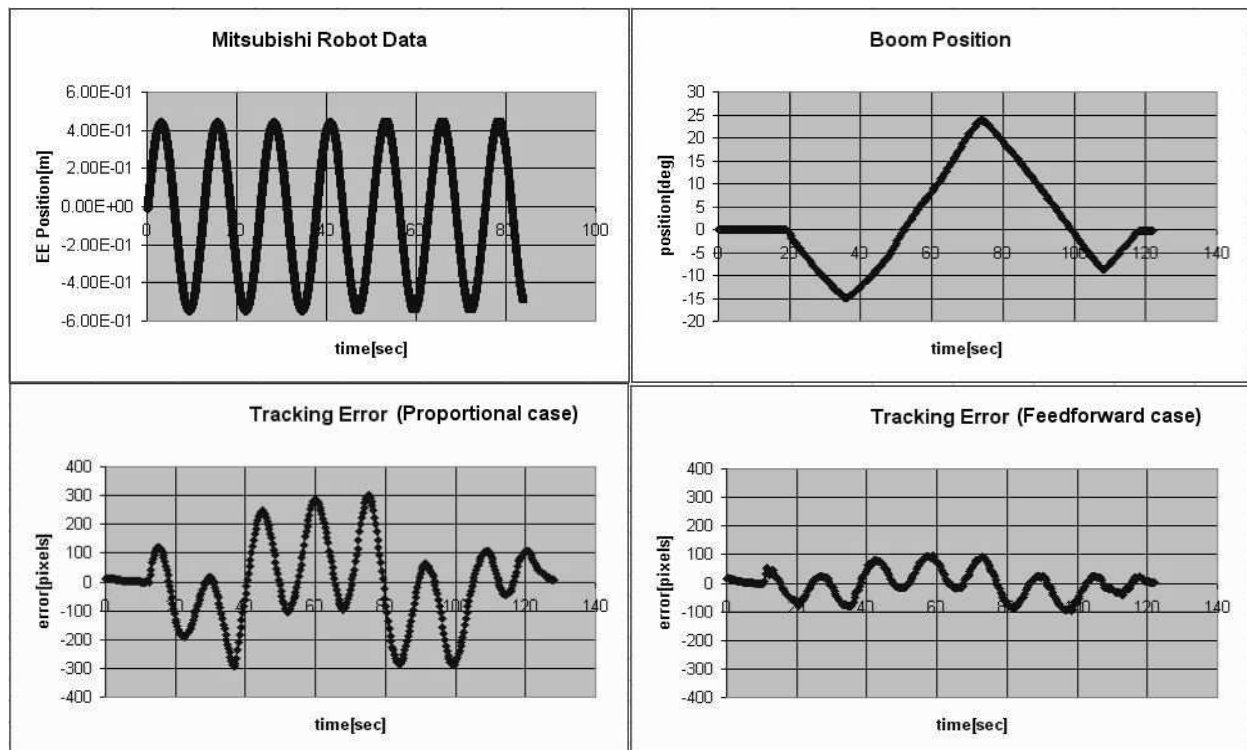


Fig. 9. Tracking errors comparing feedforward and proportional control in *human-in-the-loop visual servoing*. (top row) Target sinusoidal motion and booming. It can be seen that the operator moved the boom real slow (about $1^\circ/\text{sec}$). (bottom row) Tracking error using a proportional control (left-hand side) and a feedforward control (right-hand side). The image dimensions are 640×480 pixels.

The experiment was set up in the laboratory. The camera-target distance was 3.15 m. The target dimensions were $8.9 \times 8.25 \text{ cm}^2$. The robotic arm moved the target sinusoidally with a frequency of about 0.08 Hz and a magnitude of 0.5 m. CONDENSATION algorithm was employed for the target detection. As this algorithm is noisy, the target image should be kept small. The target dimensions in the image plane were 34×32 pixels. While both the controllers attempted to track, the boom was manually moved from -15° to $+25^\circ$. The plots can be seen in Figure 9. In the top row, the target motion and the booming plot (both versus time) can be seen. The operator moved the boom really slow (approximately $1^\circ/\text{sec}$). This booming rate was used because of the proportional controller. The tracking errors are shown in the bottom row. The bottom left image shows the error when using the proportional controller for tracking. The bottom right image shows the error when using the feedforward controller. The peak-to-peak error was about 100 pixels with the feedforward controller, while the proportional controller yielded an error of more than 300 pixels. By comparing the error in the same conditions, the conclusion was that the feedforward controller is „much better“ than the proportional controller. Still, considering that the focal length was about 1200 pixels and given the camera-target distance of 3.15 m, 100 pixels represented about 35 cm of error. This value was considered to be too big.

3.4 Symbolic model formulation and validation

At this point, a model was desired for the boom-camera system. Simulation of new controllers would be much easier once the model was available. With satisfactory simulation results, a suitable controller can be implemented for experiments.

Both the nonlinear mathematical and simulation models of the boom were developed using *Mathematica* and *Tsi ProPac* (Kwatny & Blankenship, 1995); (Kwatny & Blankenship, 2000). The former is in Poincaré equations enabling one to evaluate the properties of the boom and to design either a linear or a nonlinear controller. The latter is in the form of a C-code that can be compiled as an S-function in SIMULINK. Together, these models of the highly involved boom dynamics facilitate the design and testing of the controller before its actual implementation. The boom, shown in Figure 10, comprises of seven bodies and eight joints.

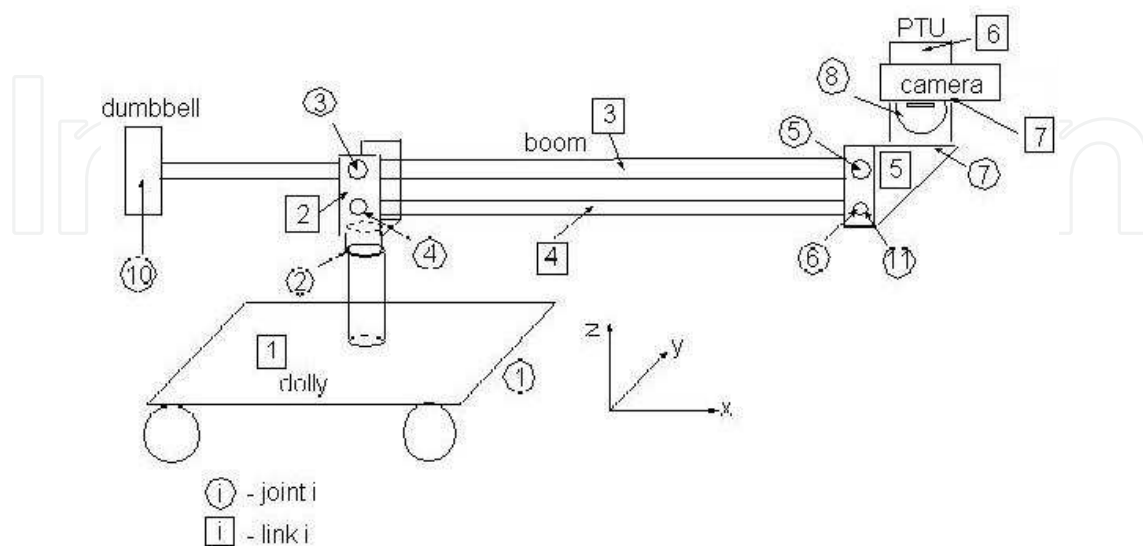


Fig. 10. Number assigned to every link and joint. *Circled numbers* represent joints while numbers in *rectangles* represent links.

| Joint # | RB | JB | x | y | R_x | R_y | R_z |
|---------|----|----|---|---|-------|----------------|----------|
| 1 | | 1 | x | y | | | |
| 2 | 1 | 2 | | | | | ψ_b |
| 3 | 2 | 3 | | | | θ_{bt1} | |
| 4 | 2 | 4 | | | | θ_{bb1} | |
| 5 | 3 | 5 | | | | θ_{bt2} | |
| 6 | 4 | 5 | | | | θ_{bb2} | |
| 7 | 5 | 6 | | | | | ψ_c |
| 8 | 6 | 7 | | | | θ_c | |

Table 1. Types of motion for links.

| Object | Mass [kg] | Moment of inertia [$kg \cdot m^2$] |
|-----------------|-----------|--|
| Dolly (link 1) | 25 | $I_{xx} = 2.48$ $I_{yy} = 0.97$ $I_{zz} = 3.465$ |
| Link 2 | 0.6254 | $I_{xx} = 0.000907$ $I_{yy} = 0.000907$ $I_{zz} = 0.00181$ |
| Boom (link 3) | 29.5 | $I_{xx} = 0$ $I_{yy} = 16.904$ $I_{zz} = 16.904$ |
| Link 4 | 0.879 | $I_{xx} = 0$ $I_{yy} = 0.02379$ $I_{zz} = 0.02379$ |
| Link 5 | 3.624 | $I_{xx} = 0.08204$ $I_{yy} = 0.00119$ $I_{zz} = 0.00701$ |
| PTU (link 6) | 12.684 | $I_{xx} = 0.276$ $I_{yy} = 0.234$ $I_{zz} = 0.0690$ |
| Camera (link 7) | 0.185 | $I_{xx} = 0$ $I_{yy} = 1.33 \cdot 10^{-5}$ $I_{zz} = 1.33 \cdot 10^{-5}$ |

Table 2. Boom links, masses, and moments of inertia.

The bodies and joints are denoted by boxes and circles, respectively. The DOFs of various joints are detailed in Table 1, while the physical data are given in Table 2. They give the position or Euler angles of the *joint body* (JB) with respect to the *reference body* (RB). At the origin, which corresponds to a stable equilibrium, the boom and the camera are perfectly aligned. One characteristic of the boom is that it always keeps the camera's base parallel to the floor. This is because bodies 3 and 4 are part of a four-bar linkage. There are two constraints for the system which can be seen in equation 9

$$\begin{aligned} \theta_{bb1} - \theta_{bt1} &= 0 \\ \theta_{bt1} + \theta_{bt2} &= 0 \end{aligned} \quad (9)$$

The inputs acting on the system are the torques Q_1 (about y) and Q_2 (about z) exerted by the operator, and the torques Q_3 and Q_4 applied by the pan and tilt motors of the camera, that is, $u = \{Q_1, Q_2, Q_3, Q_4\}$. The dumbbell at the end of body 3 is pushed to facilitate the target tracking with the camera. In this analysis, it is assumed that the operator does not move the cart, although it is straightforward to incorporate that as well. The pan and tilt motors correspond to the rotations ψ_c and θ_c , respectively.

The model can be obtained in the form of Poincaré equations [see (Kwatny & Blankenship, 1995) and (Kwatny & Blankenship, 2000) for details].

$$\begin{aligned}\dot{q} &= V(q)p \\ M(q)\dot{p} + C(q)p + Q(p, q, u) &= 0\end{aligned}\quad (10)$$

The generalized coordinate vector q (see Table 1 for notation) is given by

$$q = [x, y, \psi_b, \theta_{bt1}, \theta_{bt2}, \theta_{bb1}, \theta_{bb2}, \psi_c, \theta_c]^T \quad (11)$$

Vector p is the 7×1 vector of quasi-velocities given by

$$p = [\Omega_{yc}, \Omega_{zc}, \Omega_{bb2}, \Omega_{bt2}, \Omega_{zb}, v_y, v_x]^T \quad (12)$$

They are the quasi-velocities associated with joints 8, 7, 6, 5, 2, and a double-joint 1, respectively. The first set of equations are the kinematics and the second are the dynamics of the system.

3.5 Model validation

The simulation model is generated as a C-file that can be compiled using any standard C-compiler. The MATLAB function *mex* is used to compile it as a dll file, which defines an S-function in SIMULINK. To ascertain the fidelity of the model, the experimental results in (Stanciu & Oh, 2004) were simulated in SIMULINK. The experimental setup is depicted in Figure 3(b). The booming angles, the target motion, and the errors are shown in Figures 11 and 12, respectively. In spite of the fact that the dynamics of the wheels and the friction in the joints are neglected, the experimental and simulated results show fairly good agreement.

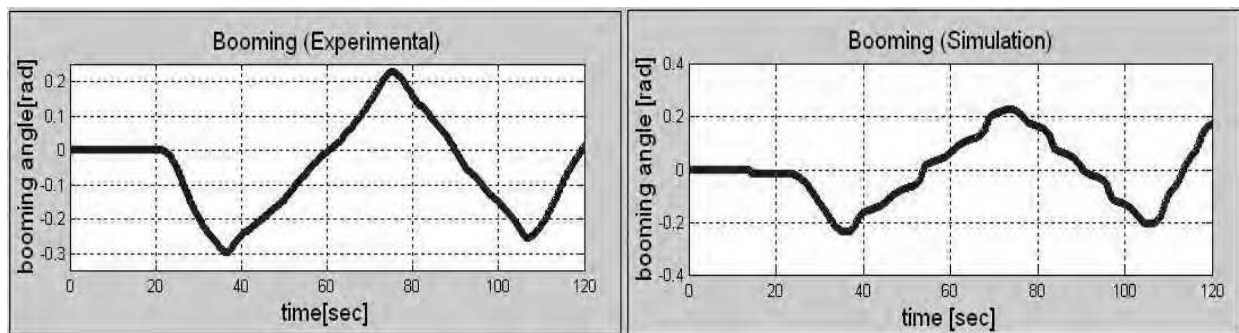


Fig. 11. Booming. Experiments (*left*) and simulation (*right*).

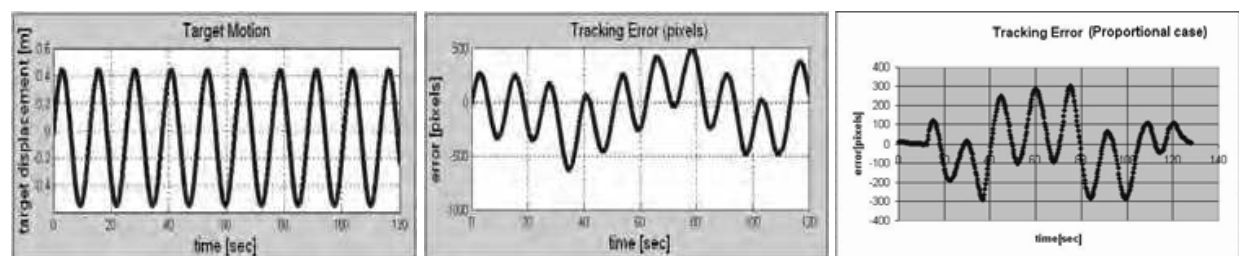


Fig. 12. Target motion (*left*). Simulation and experimental errors in pixels (central and right).

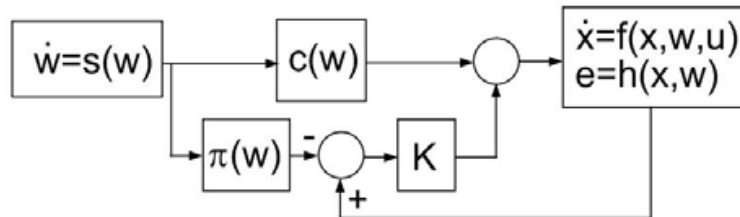


Fig. 13. Output tracking regulation controller as it was implemented.

3.6 Output Tracking Regulation Controller (OTR)

The target position in the image plane is a time-dependent function. By applying the Fourier theory, such a function can be expressed as a sum of sinusoids with decaying magnitudes and increasing frequencies. If the controller can be fine-tuned to ensure lower frequency sinusoids tracking, then the tracking error will be acceptable. The last of our hypotheses was that *adding such a controller to our system will improve the performance by reducing the error to ± 50 pixels (50%) in case of the Mitsubishi Robot experiment.*

This paper investigated the effectiveness and advantages of the controller implemented as a regulator with disturbance rejection properties. This approach guarantees regulation of the desired variables, while simultaneously stabilizing the system and rejecting the exogenous disturbances. As a first step, a linear controller was designed to regulate only the pan motion. Its structure can be seen in Figure 13. The linearized equations are recast as

$$\begin{aligned} \dot{x} &= Ax + Pw + Bu \\ \dot{w} &= Sx \\ e &= Cx + Qw \end{aligned} \quad (13)$$

The regulator problem is solvable if and only if Π and Γ satisfy the linear matrix equations 14 [(Kwatny & Kalnitsky, 1978); (Isidori 1995)]:

$$\begin{aligned} \Pi S &= A\Pi + P + B\Gamma \\ 0 &= C\Pi + Q \end{aligned} \quad (14)$$

A regulating control can, then, be constructed as

$$u = \Gamma w + K(x - \Pi w) \quad (15)$$

where K is chosen so that the matrix $A + BK$ has the desired eigenvalues. These eigenvalues determine the quality of the response. The PTU motor model has the transfer function

$$\frac{\theta(s)}{V_a(s)} = \frac{0.01175}{1.3s^2 + 32s} \quad (16)$$

where the output is the camera angle. In this case, the state space description of the system is given by matrices A , B , and C

$$\begin{aligned}
 A &= \begin{bmatrix} -24.61 & 0 \\ 1 & 0 \end{bmatrix} \\
 B &= \begin{bmatrix} 0.0088 \\ 0 \end{bmatrix} \\
 C &= [0 \quad 1]
 \end{aligned} \tag{17}$$

From equations (14)

$$\begin{aligned}
 \Pi &= \begin{bmatrix} 1 & 0 \\ 0 & 1 \end{bmatrix} \\
 \Gamma &= [-113.6 \quad 2796.6]
 \end{aligned} \tag{18}$$

The matrix K was

$$K = [-10000 \quad -380] \tag{19}$$

3.7 Simulation and experiments using output tracking regulation controller

Prior to the implementation experiment, a new controller was simulated using MATLAB SIMULINK. Sinusoidal reference signals corresponding to 1, 5, and 10 rad/sec were applied to the controller (in simulation). Both the reference and the output of the system were plotted on the same axes frame. The plots corresponding to the 5 rad/sec input can be seen in Figure 14. After the implementation, several experiments were performed using this controller. First, the controller was tested with the Mitsubishi robotic arm for a comparison of the performance of the feedforward and proportional controllers. In the second experiment, the system attempted to track a ball kicked by two players.

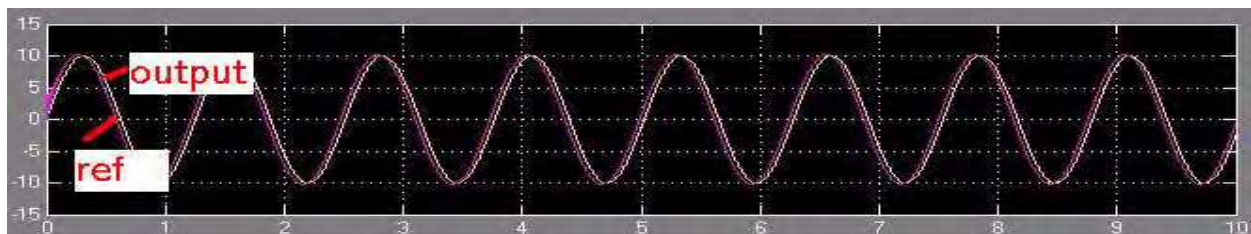


Fig. 14. Reference (5 rad/sec) as well as the output of the PTU using the new controller (the horizontal axis represents time in seconds).

In the first experiment, the robotic arm was instructed to sinusoidally move the target with the same frequency and magnitude as in the case of the feedforward controller. The camera tracked the target while the operator boomed. The booming data and the tracking error were recorded. The plots can be seen in Figure 15. In this figure, the top left plot represents the target motion while the top right plot shows the operator booming. It can be seen that the booming takes place with a frequency of about $3^\circ/\text{sec}$ (when comparing the proportional and the feedforward controllers, the booming speed was about $1^\circ/\text{sec}$). The bottom left plot is the horizontal error when using the OTR controller (provided for comparison). It can be seen that when the OTR controller is used, the error becomes ± 50 pixels (half of the value obtained using only the feedforward controller).

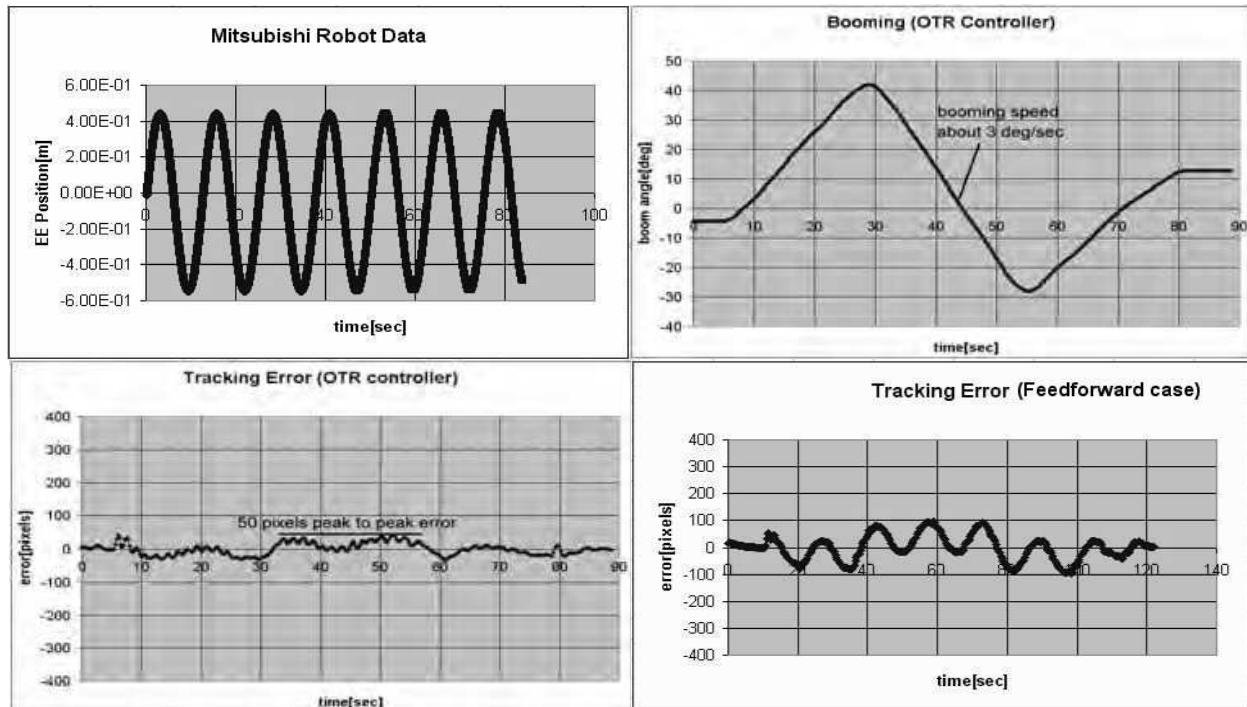


Fig. 15. Mitsubishi experiment using the OTR controller. The first figure shows the moving target. The second figure shows the boom motion. The third figure shows the tracking error in case of the output tracking controller. The fourth figure shows the error using the feedforward controller. It can be seen that by using the OTR controller, the error is less than ± 50 pixels. This value reflects a gain in performance of 50%.

3.8 Ball-tracking experiment

Since the tracking error reduced when the robotic arm was used, it was interesting to see its behavior in a more natural environment. This time the task was to track a ball moving between two players. The experiment was set up in the laboratory and videotaped using three cameras. Sequential pictures can be seen in Figure 16. The top row shows the operator booming as the camera tracks the ball. The bottom row shows the boom camera point of view. It can be seen that the target is precisely detected and tracked. Despite its „not so scientific nature“ (no data was recorded), this experiment highlighted one challenge. If the ball is kicked softly, the image processing algorithm will successfully detect it and the camera is able to track it. If the ball is kicked harder, the camera fails to track it. This means that at a frequency of 3-4 Hz (the total time to process a frame and compute the controller outputs was around 340 ms), the target acceleration is limited to small values. This particular challenge was not revealed by experiments involving the robotic arm.

4. Human versus human-vision control: a comparison

It was interesting to determine if and how this system is able to help the operator. To assess the increase in performance due to the vision system, an experiment was set up. Again, the Mitsubishi robot was used. Its end-effector moved the target on a trajectory corresponding to a figure „8“ for 60 sec. An experienced operator and a beginner were asked to handle the boom with and without the help of vision. When vision was not used, the operator manually controlled the camera using a joystick.

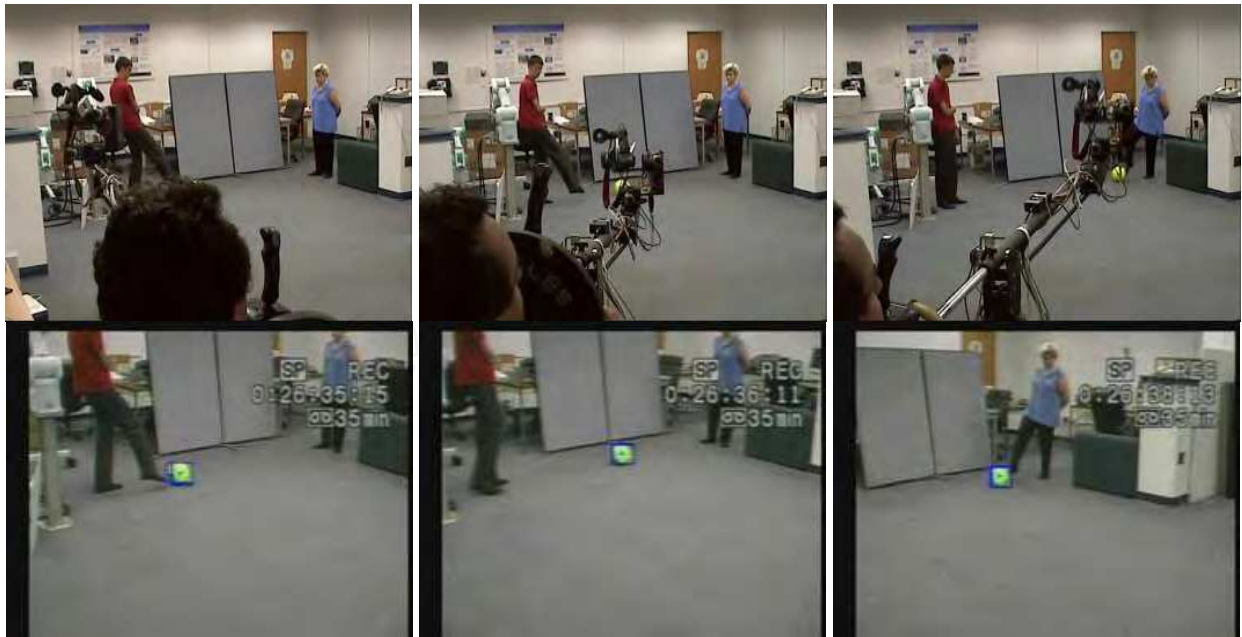


Fig. 16. Ball-tracking experiment. Operator booming and camera point of view (*top row*). Program working (*bottom row*).

A booming path was set up in an attempt to increase the experiment repeatability [shown in Figure 3(c)]. Each operator boomed two times: first, when using the vision system, and second, when manually manipulating the camera using a joystick. The objective was to keep the target in the camera's field-of-view while both the target and boom move. Several positions of interest were marked along the booming path using numbers [see Figure 3(c)]. Tracking error was recorded when using vision. Under the manual manipulation experiment, both the operators lost the target. When the target was outside the image plane, the image processing algorithm focused on other objects in the image. Because of this, the tracking error had no relevance during manual manipulation.

Sequential images from the experiment can be seen in Figures 17-20. The images are taken when the camera was in one of the positions marked in Figure 3(c).



Fig. 17. Unexperienced operator with the vision system.

In the case of using the vision system, the target was never lost (Figures 17 and 19). Moreover, the output regulation controller (which is implemented for the pan motion) maintains the target very close to the image center.

In the case of manual tracking (Figures 18 and 20), the operator has to manipulate the boom as well as the camera. It can be seen that both the operators have moments when the target is lost. In case of an unexperienced operator without vision, the booming took longer than the motion of the robotic arm simply because there are more DOFs to be controlled simultaneously. The unexperienced operator lost the target eight times. The experienced operator was able to finish booming within 60 sec, but he lost the target five times. Because the program focuses on something else in the absence of the target, the data regarding the tracking error is not relevant when the target was lost. The target was never lost when using vision. The absolute value of the error in both the cases is shown in Figure 21. One can see that the values are in the same range. This means that visual servoing helps the novice operator to obtain performance similar to that of the expert.



Fig. 18. Unexperienced operator without the vision system. The target was lost eight times. The pictures were taken when the camera was in positions of interest shown in Fig. 3(c) and the top row of Fig 17. Because the target was lost, the tracking error curve has no relevance.



Fig. 19. Experienced operator with the vision system. Again, target is never lost. The pictures were taken when the camera was in positions of interest shown in Fig. 3(c) and the top row of Fig. 17.



Fig. 20. Experienced operator without the vision system. The target was lost five times. Because the target was lost, the tracking error curve has no relevance. The pictures were taken when the camera was in positions of interest shown in Fig. 3(c) and the top row of Fig. 17.

5. Conclusion and future work

This paper integrates visual-servoing for augmenting the tracking performance of camera teleoperators. By reducing the number of DOFs that need to be manually manipulated, the

operator can concentrate on coarse camera motion. Using a broadcast boom system as an experimental platform, the dynamics of the boom PTU were derived and validated experimentally. A new controller was added to the feedforward scheme and tested experimentally. The performance of the new control law was assessed by comparing the use of the vision system versus manual tracking for both an experienced and an unexperienced operator. The addition of the OTR controller to the feedforward scheme yielded lower errors. The use of the vision system helps the operator (the target was precisely detected and tracked). This suggests that by using the vision system, even an unexperienced operator can achieve a performance similar to that of a skilled operator. Also, there are situations when vision is helpful for a skilled operator. Still, there are situations when the target detection and tracking fail. A mechanism to detect such situations and alert the operator is desirable. When such situations occur, the camera can be programmed to automatically move to a particular position. The ball-tracking experiment proves to be successful if the ball is hit softly. When the ball is hit harder, the image processing fails to detect it, and tracking fails. However, there is no proof that controllers would be able to track a harder-hit ball if image processing did not fail.

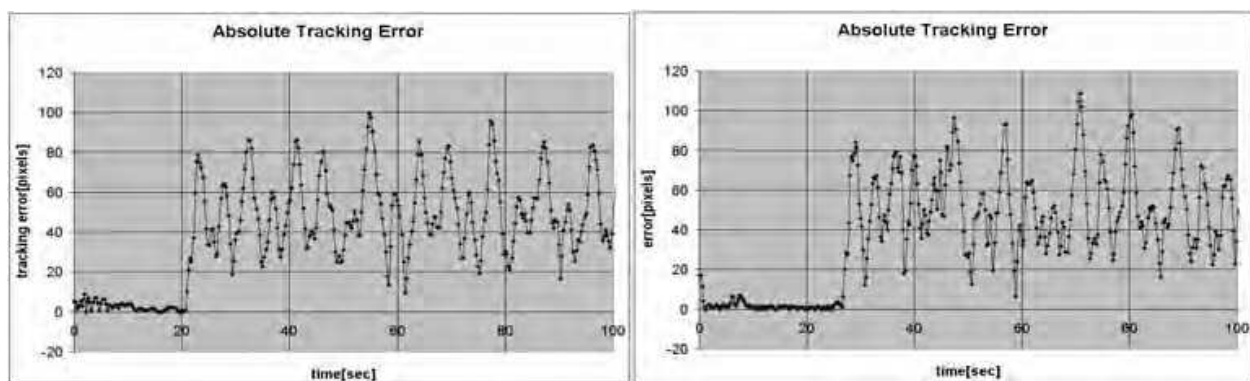


Fig. 21. Tracking error. Experienced operator with vision (*left-hand side*). Unexperienced operator using vision (*right-hand side*). Booming path was restricted. It can be seen that there are no significant differences between these two plots.

Another case that is not investigated in this paper is occlusion. Such experiments were not performed. They should be studied in future work. Because the focus of this research was the control part, the case of appearance of similar targets in the image plane was not studied. The effect of the image noise, when the camera moves quickly was also not studied. Future work will also have to focus on increasing tracking performance. If this tracking system is to be used in sports broadcasting, it will have to be able to track objects moving with higher acceleration. The sampling time (which now corresponds to 3-4 Hz) will have to decrease (perhaps one way to achieve this is to use a faster computer). When tracking sports events (football, soccer, etc.), when the target moves with high accelerations and its dimensions vary in the image, a target estimation mechanism will be desirable. Such a mechanism would record ball positions and estimate its trajectory. Once the estimation is done, this mechanism would command the camera to move to the estimated „landing“ position and try to re-acquire the ball. Combining this mechanism with zooming in and out would allow tracking of faster objects.

6. References

- Corke P.I.; Good M.C. (1996). Dynamic effects in visual closed-loop systems. *IEEE Trans. Robot. Autom.* Vol. 12, No. 5, Oct 2001, pp. 671-683,
- Ferrier N. (1998). Achieving a Fitts Law relationship for visual guided reaching. *Proceedings of Int. Conf. Comput. Vis. (ICCV)* pp. 903-910 Bombay, India, Jan. 1998,
- Fitts P. M. (1954). The information capacity of the human motor system in controlling the amplitude of movement. *J. Exp. Psychology*, Vol. 47, No. 6, 1954, pp. 381-391,
- Hutchinson S., Hager G.D., Corke P.I. (1996). A tutorial on visual servo control. *IEEE Trans. Robot. Autom.* pp. 651-670, Vol.12, No. 5, Oct. 1996,
- Hill J., Park W.T. (1973). Real time control of a robot by visual feedback in assembling tasks. *Pattern Recognit* Vol. 5 pp. 99-108, 1973,
- Isard M., Blake A. (1998). CONDENSATION - Conditional density propagation for visual tracking. *Int. J. Comput. Vis.*, Vol. 29, No. 1, pp. 5-28, 1998,
- Isidori A. (1995) *Nonlinear Control Systems* 3rd ed. Springer-Verlag, 3-540-19916-0, New York,
- Kalata P.R., Murphy K.M. (1997). $\alpha - \beta$ target tracking with track rate variations. *Proceedings of 29th Southeastern Symp. Syst. Theory*, pp. 70-74, Mar. 1997,
- Kwatny H.G., Kalnitsky K.C. (1978). On alternative methodologies for the design of robust linear multivariable regulators. *IEEE Trans. Autom. Control*, Vol. AC-23, No. 5, Oct. 1978, pp. 930-933,
- Kwatny H. G., Blankenship G.L. (1995). Symbolic construction of models for multibody dynamics. *IEEE Trans. Robot. Autom.*, Vol. 11, No. 2, Apr. 1995 pp. 271-281,
- Kwatny H. G., Blankenship G.L. (2000). *Nonlinear Control and Analytical Mechanics: A Computational Approach*, Birkhauser, 0-8176-4147-5, Boston, MA,
- Oh P. Y., Allen P. K. (2001). Visual servoing by partitioning degrees of freedom. *IEEE Trans. Robot. Autom.* Vol. 17 No. 1, , Feb. 2001, pp. 1-17,
- Oh P. Y. (2002). Biologically inspired visual-servoing using a macro/micro actuator approach. *Int. Conf. Imaging Sci., Syst. Technol (CISST)*, Jun 2002 Las Vegas CA,
- Papanikolopoulos N.P., Khosla P.K., Kanade T. (1993). Visual tracking of a moving target by a camera mounted on a robot: A combination of vision and control. *IEEE Trans. Robot. Autom.*, Vol. 9, No. 1, Feb. 1993, pp. 14-35,
- Sanderson A.C., Weiss L.E. (1980). Image-based visual servo control using relational graph error signals. *Proceedings of IEEE Int. Conf. Robot. Autom.*, 1980, pp. 1074-1077,
- Sheridan T.B., Ferrell W.R. (1963). Remote manipulative control with transmission delay. *IEEE Trans. Human Factors in Electronics* Vol. HFE-4, 1963, pp. 25-29,
- Stanciu R., Oh P.Y. (2002). Designing visually servoed tracking to augment camera teleoperators. *Proceedings of IEEE Int. Conf. Intell. Robots Syst. (IROS)*, Vol. 1, Lausanne, Switzerland, 2002, pp. 342-347,
- Stanciu, R., Oh, P.Y. (2003). Human-in-the-loop visually servoed tracking. *Proceedings of Int. Conf. Comput. Commun. Control Technol. (CCCT)*, Vol. 5, pp. 318-323, Orlando, FL, Jul. 2003,
- Stanciu R., P.Y. Oh P.Y. (2004), Feedforward control for human-in-the-loop camera systems. *Proceedings of Int. Conf. Robot. and Autom. (ICRA)*, Vol. 1, pp. 1-6, New Orleans, LA, Apr. 2004,
- Tenne D., Singh T. (2000). Optimal design of $\alpha - \beta - (\gamma)$ filters. *Proceedings of Am. Control Conf.*, Vol. 6, pp. 4348-4352, Chicago, Illinois, Jun. 2000.



Visual Servoing

Edited by Rong-Fong Fung

ISBN 978-953-307-095-7

Hard cover, 234 pages

Publisher InTech

Published online 01, April, 2010

Published in print edition April, 2010

The goal of this book is to introduce the visual application by excellent researchers in the world currently and offer the knowledge that can also be applied to another field widely. This book collects the main studies about machine vision currently in the world, and has a powerful persuasion in the applications employed in the machine vision. The contents, which demonstrate that the machine vision theory, are realized in different field. For the beginner, it is easy to understand the development in the vision servoing. For engineer, professor and researcher, they can study and learn the chapters, and then employ another application method.

How to reference

In order to correctly reference this scholarly work, feel free to copy and paste the following:

Rares Stanciu and Paul Oh (2010). Human-in-the-Loop Control for a Broadcast Camera System, Visual Servoing, Rong-Fong Fung (Ed.), ISBN: 978-953-307-095-7, InTech, Available from:

<http://www.intechopen.com/books/visual-servoing/human-in-the-loop-control-for-a-broadcast-camera-system>

INTECH
open science | open minds

InTech Europe

University Campus STeP Ri
Slavka Krautzeka 83/A
51000 Rijeka, Croatia
Phone: +385 (51) 770 447
Fax: +385 (51) 686 166
www.intechopen.com

InTech China

Unit 405, Office Block, Hotel Equatorial Shanghai
No.65, Yan An Road (West), Shanghai, 200040, China
中国上海市延安西路65号上海国际贵都大饭店办公楼405单元
Phone: +86-21-62489820
Fax: +86-21-62489821

© 2010 The Author(s). Licensee IntechOpen. This chapter is distributed under the terms of the [Creative Commons Attribution-NonCommercial-ShareAlike-3.0 License](#), which permits use, distribution and reproduction for non-commercial purposes, provided the original is properly cited and derivative works building on this content are distributed under the same license.

IntechOpen

IntechOpen